UCRL-JC-132065
PREPRINT

Thermomechanical Effects on Permeability for a 3-D Model of YM Rock

P.A. Berge
S.C. Blair
H.F. Wang

This paper was prepared for submittal to the
37th U.S. Rock Mechanics Symposium
Vail, CO
June 6-9, 1999

January 15, 1999

Thermomechanical effects on permeability for a 3-D model of YM rock

P.A. Berge, S.C. Blair
Lawrence Livermore National Laboratory, USA
H.F. Wang
University of Wisconsin–Madison, USA

ABSTRACT: We estimate how thermomechanical processes affect the spatial variability of fracture permeability for a 3-D model representing Topopah Spring tuff at the nuclear-waste repository horizon in Yucca Mountain, Nevada. Using a finite-difference code, we compute thermal stress changes. We evaluate possible permeability enhancement resulting from shear slip along various mapped fracture sets after 50 years of heating, for rock in the near-field environment of the proposed repository. Our results indicate permeability enhancement of a factor of 2 for regions about 10 to 30 m above drifts, for north–south striking vertical fractures. Shear slip and permeability increases of a factor of 4 can occur in regions just above drifts, for east–west striking vertical fractures. Information on how permeability may change over the lifetime of a geologic repository is important to the prediction and evaluation of repository performance.

1 INTRODUCTION

This paper describes current results for modeling geomechanical behavior of the Topopah Springs tuff in the near-field environment (NFE) of the potential repository at Yucca Mountain, Nevada. The modeling focuses on estimating how thermomechanical (TM) processes affect the spatial variability of fracture permeability. A more detailed description of the method and our modeling is given in Berge et al. (1998). Our results were obtained by a thermohydromechanical (THM) modeling procedure (i.e. modeling coupled thermohydrologic [TH] and TM processes). These results are needed for modeling changes in repository-level moisture movement and thermally induced seepage and for assessment of rock fall and tunnel collapse.

Specifically, we used the TM three-dimensional (3-D) finite-difference code Fast Lagrangian Analysis of Continua in 3 Dimensions (FLAC^{3D}) version 2.0 (Itasca Consulting Group Inc. 1997) to compute changes in stress and displacement in an elastic model subjected to temperature changes over time. Output from TH modeling (Hardin et al. 1998, Chapter 3) using the code Nonisothermal Unsaturated–Saturated Flow and Transport (NUFT) (Nitao 1998a, 1998b) provided the temperature changes for input to FLAC^{3D}. We then estimated how the stress changes could affect permeability.

By using a model based on the work of Barton et al. (1997, 1995) and the Mohr–Coulomb criterion (Jaeger & Cook 1976, p. 399), we determined which regions of the model would experience increases in permeability because of shear slip along fractures having particular orientations. As done in our previous work (Blair et al. 1997) incorporating a model developed by Brown (1994, 1995, Brown & Bruhn 1997), we estimated that the permeability would increase by approximately a factor of two for regions where shear slip could occur along parallel fractures. If slip occurred along two different fracture sets, the permeability could increase by a factor of at least four.

2 METHOD

2.1 *The model*

Setting up a TM model for FLAC^{3D} requires defining a grid, setting mechanical and thermal initial and boundary conditions, choosing appropriate constitutive models, and assigning material properties to each zone in the grid.

For this paper, we chose to base our 3-D THM modeling on a coarser version of the 2-D model we ran for the work described in a Yucca Mountain/LLNL report (Hardin et al. 1998, Chapter 4). The grid and temperature field were based on those used by the TH code for 50 years of heating for the reference Case 1 TH model calculated using Total System Performance Assessment—Viability Assessment (TSPA–VA) base-case properties, nominal infiltration, and a point-load repository design (Hardin et al. 1998, Chapter 3).

The model (Figure 1) uses three drifts, centered at a depth of 385 m in a model extending from 337 m depth to 431.8 m depth; because the problem is symmetrical, only 1.5 drifts are actually modeled, and the plane at $x = 0.0$ is a symmetry plane. The model, which has 3240 zones, represents the drifts and two Topopah Spring tuff units, geological units Tptpll and Tptpmn.

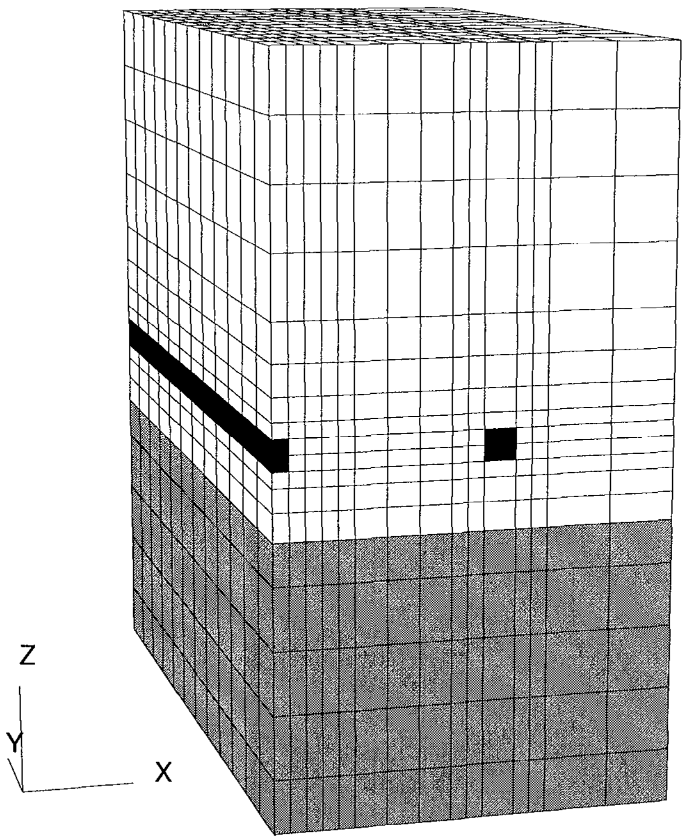

Figure 1. Model for 1.5 drifts in 3-D, model geometry; darkest regions indicate drift locations. Drifts are 4 m high.

To maximize stresses and to reduce the number of required rock properties to the simplest case, the elastic–isotropic constitutive model was used in all zones. The model properties used for the tuff (Table 1) are consistent with the unsaturated zone (UZ) site-scale model (Bodvarsson & Bandurraga 1996, Bodvarsson et al. 1997).

Table 1. Rock properties

Unit	Tptpmn	Tptpll	Drifts
Bulk Modulus (GPa)	19.	16.	8.
Shear Modulus (GPa)	14.	11.	6.
Density (kg/m^3)	2300.	2300.	2000.
Thermal Conductivity (W/m·K)	1.2	1.4	1.2
Specific Heat (J/kg·K)	900.	870.	900.
Thermal-Expansion Coefficient (K^{-1})	$10. \times 10^{-6}$	$10. \times 10^{-6}$	$10. \times 10^{-6}$

The moduli values listed in Table 1 have uncertainties of approximately ±3 to 4 GPa. Using different values for the bulk and shear moduli would not greatly affect our main results. The results are much more sensitive to the thermal-expansion coefficient, which is known to vary with temperature by a factor of 3 or 4 (Bodvarsson & Bandurraga 1996, Bodvarsson et al. 1997). For this paper, we used a thermal-expansion coefficient appropriate for temperatures of about 25°C (298 K) to 175°C (448 K) (Bodvarsson & Bandurraga 1996, Bodvarsson et al. 1997). Future modeling will include parameter sensitivity studies for the thermal-expansion coefficient.

The thermal conductivity and specific heat are not actually used in the FLAC^{3D} modeling because the temperature field is computed by the NUFT code (Hardin et al. 1998, Chapter 3) instead of by FLAC^{3D}. The values in Table 1 for thermal conductivity and specific heat were those used by NUFT.

The TH code NUFT is described in detail by Nitao (1998a, 1998b). This code is an integrated suite of numerical models for flow and transport in porous media. It can model multiphase flow in both the vadose and saturated zones and can model heat transfer by mass advection, diffusion, and thermal conduction. Complex processes such as drying and rewetting are accommodated by the dynamic switching of primary variables that NUFT is capable of performing. The highly sophisticated temperature calculations from NUFT are preferred to using the simple thermal modeling of the mechanical code FLAC^{3D} for computing the temperature.

For the mechanical initial and boundary conditions in our FLAC^{3D} modeling, we fixed the bottom of the model in all directions and fixed the symmetry plane in the x direction. We applied a lithostatic szz stress to the top of the model and applied horizontal stresses sxx and syy about half as large to the sides of the model. This corresponds to an assumption of a Poisson's ratio of 1/3, which may be slightly high, but is not expected to affect our results significantly and is certainly correct to the first order. We used a gravitational gradient for all applied stresses and set initial stresses in all zones to be in equilibrium with these applied stresses; initially, sxx = syy = 4.85 MPa in compression near top of model, with vertical gradient of 0.0115 MPa/m; szz = 7.6 MPa at the top of the model with a vertical gradient of 0.023 MPa/m, so that the bottom zones have szz = 9.7 MPa in compression. These stress values are consistent with available in situ stress data (Stock et al. 1984, 1985).

We allowed all the exterior boundaries of the model to be adiabatic, including the symmetry plane boundary at $x = 0$. We used an initial temperature field with values of approximately 298 K (25°C) at the top of the model and about 299 K (26°C) at the bottom of the model. These temperatures came from the initial temperatures used in NUFT modeling (Hardin et al. 1998, Chapter 3), which set the surface temperature at 15.8°C and used a temperature of 34.6°C at a depth of 728.7 m at the water table.

2.2 *Calculating stress changes*

We began our THM modeling by setting up the grid and assigning material properties and initial and boundary conditions, and then brought the model to equilibrium for the initial temperature field. We set the displacements to zero in all zones once the model was in mechanical and thermal equilibrium.

We ran FLAC^{3D} in the thermal mode and read in temperatures appropriate for 50 years of heating. The temperature field is shown in Figure 2. The maximum temperature is about 420 K (147°C) in the center of a drift. Note the asymmetrical isotherms and the steep thermal gradient above the drifts. Details of the NUFT temperature calculations are in a Yucca Mountain/LLNL report (Hardin et al. 1998, Chapter 3). The asymmetrical temperature field leads to an asymmetrical stress field.

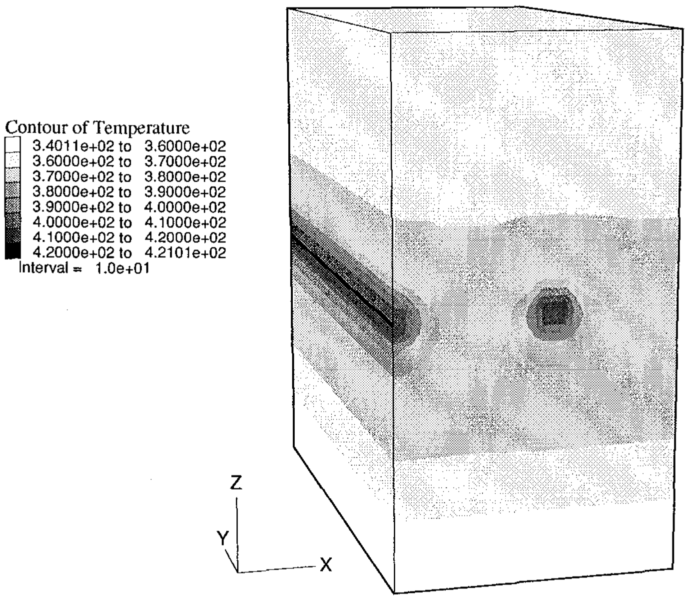

Figure 2. Temperatures (K) after 50 years of heating, from previous NUFT TH modeling

We computed thermal stresses and displacements resulting from 50 years of heating by running FLAC^{3D} in the mechanical mode and bringing the model to mechanical equilibrium. The new stress field is shown in Figure 3. The stress field has rotated in the heater region so that the principal stress directions exhibit a lot of lateral heterogeneity (in the *x* direction) below the heaters. The stresses have increased significantly compared to the initial values near 5 to 10 MPa in compression before heating.

The horizontal stresses have increased to about 15 to 20 MPa in compression near the bottom of the model (see Berge et al. 1998 for detailed plots). Horizontal stresses in the *x* direction have dropped at the top of the model and in the region midway between the drifts, to values as low as 1 MPa in compression. Values are much higher for horizontal stresses in the *y* direction and for all horizontal stresses near the heaters, about 10 MPa in the region

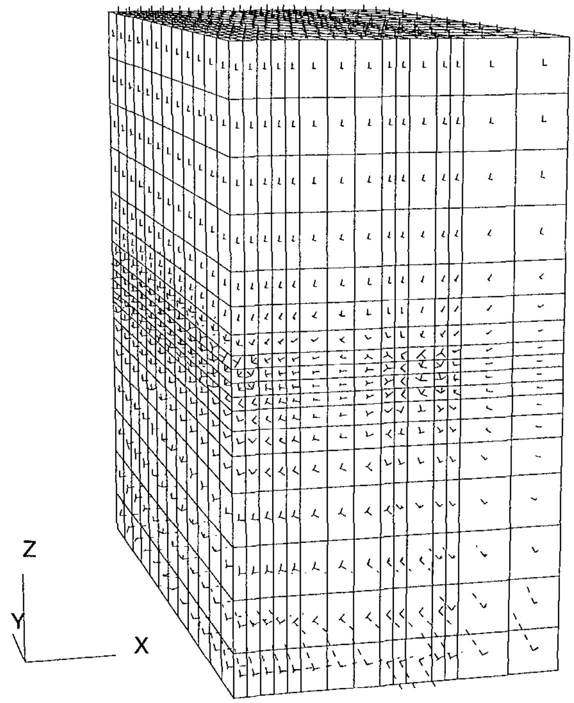

Figure 3. Model for 1.5 drifts in 3-D, stress field after 50 years of heating; maximum stress = 46 MPa

next to the drifts about two drift diameters away. The sxy and sxz shear stresses are relatively small, about 2 MPa, in most parts of the model. High syz shear stresses are found in the plane midway between the drifts where syz values reach about 5 MPa, and in the *yz* planes containing the drifts. Vertical stresses are high (10 to 20 MPa) near the top and bottom of the model. The region between drifts has high vertical stress gradients. Some artifacts, due to edge effects, can be seen in the stresses for the outermost blocks in the model. The presence of such artifacts suggests that future modeling should use boundaries that are much further away from the region of interest in the model. (To find minimum and maximum estimates for displacements, future modeling must also compare results for fixed and applied stress boundary conditions.)

2.3 *Estimating permeability changes*

The proposed-repository host rock is a fractured, densely welded, ash-flow tuff with low matrix permeability. Any changes in rock mass permeability from TM effects can be attributed to changes in the fractures because changes to matrix permeability in response to stress and temperature are small (Hardin & Chesnut 1997).

Laboratory studies (Bandis et al. 1983, Barton et al. 1985) have shown that greater impact often results from shear deformation of fractures rather than from normal deformation. Permanent changes in hydrologic properties or flow paths can result from normal deformation, but they tend to be smaller than those caused by shear displacements; this has been observed in field studies (e.g. Wilder 1987). Studies have also shown that fracture shear displacement can significantly increase fracture permeability and that the magnitude of the change may readily exceed that due to normal displacement (Barton et al. 1985). Finally, it is widely accepted that the hydrologic behavior of a fractured rock mass is controlled by relatively few, well-connected fractures.

In previous work (Blair et al. 1997, Hardin et al. 1998, Chapter 4), we used the concept of preferential flow along critically stressed fractures (Barton et al. 1997, 1995) to develop a method for determining increased permeability. We identified the regions of a 2-D FLAC model that exhibited stress conditions that would cause slip along fractures and related increases in permeability.

Barton et al. (1997) presented evidence that hydraulically conductive fractures are the fractures that are critically stressed. To estimate permeability changes due to heating, we applied this concept in our previous work (Blair et al. 1997, Hardin et al. 1998, Chapter 4) for stress fields calculated using the 2-D FLAC code.

The Mohr–Coulomb criterion is:

$$|\tau| \geq c + (fS_n)\,, \tag{1}$$

where τ is the shear stress, S_n is the compressive normal stress, c is the cohesion, and f is the coefficient of friction. The maximum potential for frictional slip occurs for a cohesion value of zero (i.e. shear offset occurs when the ratio $|\tau|/(fS_n) \geq 1$). This ratio was contoured for values greater than one for various slip planes (Blair et al. 1997, Hardin et al. 1998, Chapter 4). Thus, contoured regions were those in which the slip criterion is satisfied and shear offset is expected. Using this procedure in our previous work, we found regions of our 2-D FLAC models where slip would be expected to enhance permeability for fractures at certain angles. Although this provides an indication of the spatial distribution of permeability enhancement, more assumptions are needed to estimate the magnitude of the permeability changes.

In our previous work, we developed a method for estimating the magnitude of the permeability changes due to fracture slip (Blair et al. 1997, Hardin et al. 1998, Chapter 4). This method is based on the work of Brown (Brown 1994, 1995, Brown & Bruhn 1997). Other simple assumptions could be used to relate slip to permeability changes; this is only one possible rule. Because we used it for previous 2-D modeling, we will again apply this method. Future work will incorporate effects of increasing fracture apertures and concentrations near excavations (e.g. Ouyang & Elsworth 1993). Details of our method are in Berge et al. (1998).

As shown in Berge et al. (1998), the maximum change in permeability with this set of assumptions is that it doubles as a result of frictional slip. We therefore estimate that regions of the model in which shear slip is likely to occur along a particular set of fractures may have permeability increases of a factor of two. If slip can occur along two or more sets of fractures oriented at different angles, the permeability may increase by a factor of four or more, assuming slip is small enough that the effects of slip along another set of fractures can be added linearly.

The stress field in 3-D is considerably more complicated than in 2-D. Two rotation angles are required for relating principle stress directions to fracture orientations, and the fractures of interest may lie anywhere within the model volume. Calculating and displaying the results for the 3-D case are much more complicated than for the 2-D case.

However, some simplification is possible because most of the fractures of interest are likely to be horizontal or vertical. In general, three fracture sets have been identified in the Exploratory Studies Facility (ESF) at Yucca Mountain (Albin et al. 1997):

- Set 1 is a steeply dipping set of fractures striking east–west (EW).
- Set 2 is a steeply dipping set of fractures striking north–south (NS).
- Set 3 is a subhorizontal (H) set of fractures striking east–west.

In our modeling for this paper, we only consider vertical and horizontal fractures. Because our model is 3-D, this includes many possible fracture sets.

An additional simplifying assumption is to consider only vertical fractures that are parallel to the *xz* or the *yz* planes. This assumption is reasonable for preliminary modeling because the axis of the heated drift for the Drift-Scale Test (Blair et al. 1998) is oriented east–west; hence, EW Set 1 and H Set 3 strike perpendicular to the plane containing the drift cross section, and NS Set 2 is perpendicular to the drift axis. For our model geometry, we can assume that EW Set 1 is represented by vertical fractures parallel to the *yz* plane, NS Set 2 is represented by vertical fractures parallel to the *xz* plane, and H Set 3 is represented by horizontal fractures parallel to the *xy* plane.

Thus, the calculations of shear slip for vertical and horizontal fractures in the 3-D model can make use of equations from Turcotte and Schubert (1982, p. 82) that were used in previous 2-D modeling (see Berge et al. 1998 for details).

We used these simplifying assumptions for our initial modeling of permeability enhancement due to shear slip in the 3-D model. The same assumptions as those used in the 2-D case were applied, after we had found regions where shear slip would be expected to occur along horizontal or vertical fractures, for estimating the magnitude of the permeability change due to shear slip.

3 RESULTS

We used the procedure described in the previous section to find regions of the 3-D model where shear slip may be expected to occur along vertical or horizontal fractures. We display examples of these regions, using contour plots for the Mohr–Coulomb criterion (Jaeger and Cook 1976, p. 399), in Figure 4 and Figure 5. (Additional plots are shown in Berge et al. 1998.) Here the ratio of the shear stress to the frictional resistance for particular fractures is contoured. A ratio of one or more means that shear slip may occur in that region; a value less than one means that no slip is expected to occur.

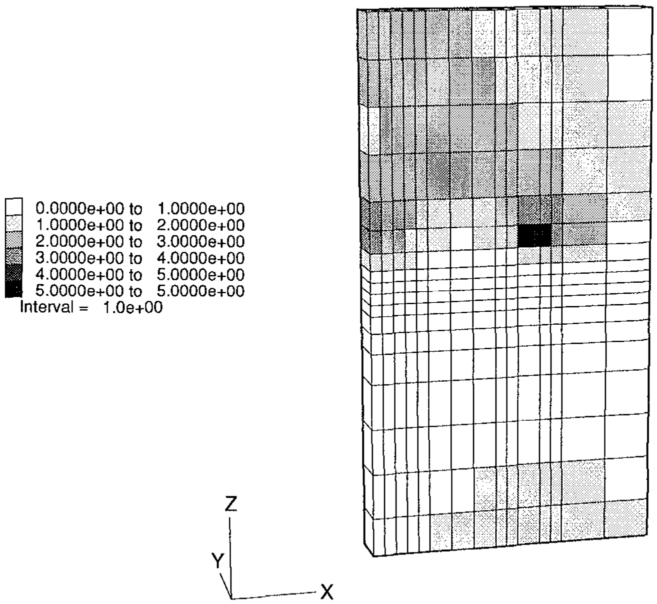

Figure 4. Contours of the ratio of shear stress to frictional resistance for slip planes parallel to the *yz* plane and cutting the *xz* plane (fracture Set 1), region near middle of model

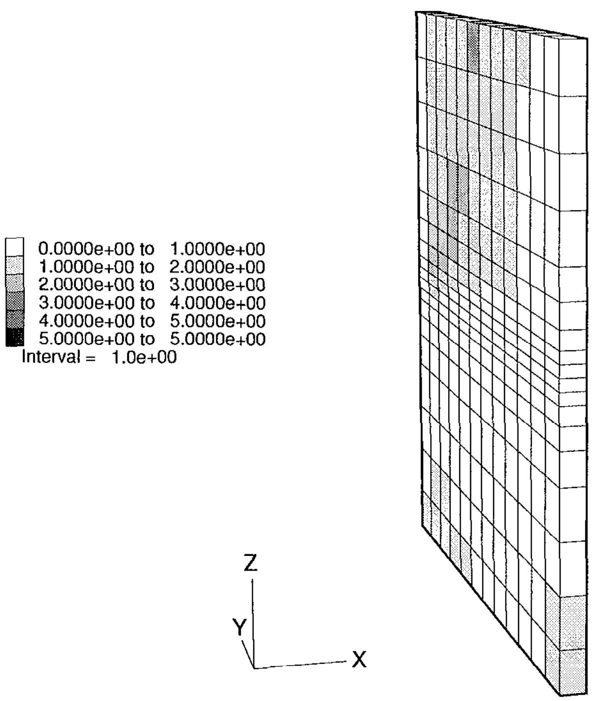

Figure 5. Contours of the ratio of shear stress to frictional resistance for slip planes parallel to the *xz* plane and cutting the *yz* plane (fracture Set 2), region midway between drifts

We plot results for fracture Set 1 (EW) in Figure 4. This figure shows that slip is quite likely for EW fracture Set 1 in most parts of the model above the drifts.

Results for slip along NS fracture Set 2 are plotted in Figure 5 for the region halfway between the drifts. These results show that slip is expected along the fractures near the top of the model in regions between the drifts. Note that the 2-D FLAC model was perpendicular to the *yz* plane and thus could not assess slip along these directions (Hardin et al. 1998, Chapter 4).

Results (not shown) for contours for EW fracture Set 1 in regions lying about 10 m above, at, and about 10 m below the drifts in our 3-D model show that slip is only expected along these fractures in regions approximately 10 m above the drifts. Results in the same regions for NS fracture Set 2 (not shown) indicate that slip may occur along fractures parallel to NS Set 2 near the drifts, but no slip is expected in regions approximately 10 m above or 10 m below the drifts.

Results for H fracture Set 3 (not shown) indicate no slip is expected along the horizontal fractures anywhere in the 3-D model.

The results show consistently that NS fracture Set 2 is likely to exhibit slip due to thermal stresses, in many parts of the model, and EW fracture Set 1 may have slip in regions just above the drifts, but H fracture Set 3 is unlikely to have any thermally induced slip. Therefore, we conclude that widespread permeability enhancement of about a factor of two is likely for fractures parallel to NS Set 2, the vertical fractures that strike north–south, for regions above the drifts. In some regions just above the drifts, permeability may increase by a factor of four if slip also occurs along the vertical fractures in EW Set 1.

4 CONCLUSIONS

We performed THM modeling to estimate bounds on permeability changes in the NFE of the proposed repository at Yucca Mountain. For our modeling, we used the TM three-dimensional (3-D) finite-difference code FLAC^{3D} version 2.0 (Itasca Consulting Group Inc. 1997) to compute changes in stress and displacement in an elastic model subjected to temperature changes over time. Output from TH modeling (Hardin et al. 1998, Chapter 3) using the code NUFT (Nitao 1998a, 1998b) provided temperature changes for input to FLAC^{3D}. We then estimated how the stress changes could affect permeability.

For this paper, we chose to base our 3-D THM modeling on a coarser version of the 2-D model we ran for the work described in a Yucca Mountain/LLNL report (Hardin et al. 1998, Chapter 4).

The grid and temperature field were based on those used by the TH code for 50 years of heating for the reference Case 1 TH model calculated using Total System Performance Assessment—Viability Assessment (TSPA–VA) base-case properties, nominal infiltration, and a point-load repository design (Hardin et al. 1998, Chapter 3).

The stress field rotated in the region between and below the drifts after 50 years of heating. High vertical shear stresses were computed for these regions.

Estimates of permeability changes were obtained by analyzing stresses, following a method we developed previously for 2-D models. In our 3-D modeling for this paper, we only considered vertical and horizontal fractures. We extended our 2-D method to a simplified 3-D case.

We conclude that widespread permeability enhancement is likely for fractures parallel to NS fracture Set 2, the vertical fractures that strike north–south, for regions above the drifts. In some regions just above the drifts, permeability may increase by a minimum of a factor of two and possibly more than a factor of four if slip also occurs along the vertical fractures in EW Set 1, the east–west fractures. Our 3-D results agree with those obtained in previous 2-D modeling, with the added advantage that we were able to model permeability changes in directions orthogonal to the 2-D model.

REFERENCES

Albin, A. L., W. L. Singleton, T. C. Moyer, A. C. Lee, R. C. Lung, G. L. W. Eatman & D. L. Barr 1997. *Geology of the Main Drift—Station 28+00 to 55+00, Exploratory Studies Facility. Yucca Mountain Project, Yucca Mountain, Nevada.* Denver: Bureau of Reclamation and U.S. Geological Survey.

Bandis, S., A. C. Lumsden & N. R. Barton 1983. Fundamentals of rock joint deformation. *Int. J. Rock Mech. Min. Sci. & Geomech. Abs*. 20:249–268.

Barton, C. A., S. Hickman, R. Morin, M. D. Zoback, T. Finkbeiner, J. Sass & D. Benoit 1997. Fracture permeability and its relationship to in-situ stress in the Dixie Valley, Nevada, geothermal reservoir. In proceedings from *Twenty-Second Workshop on Geothermal Reservoir Engineering*. January 27–29, 1997. Stanford, California: Stanford University.

Barton, C. A., M. D. Zoback & D. Moos 1995. Fluid flow along potentially active faults in crystalline rock. *Geology* 23(8):683–686.

Barton, N. R., S. Bandis & K. Bakhtar 1985. Strength, deformation, and conductivity coupling of rock joints. *Int. J. Rock Mech. Min. Sci. & Geomech. Abs*. 22(3):121–140.

Berge, P. A., H. F. Wang & S. C. Blair 1998. *Estimated bounds on rock permeability changes from THM processes.* (UCRL-ID-131492) Livermore, California: Lawrence Livermore National Laboratory.

Blair, S. C., P. A. Berge & H. F. Wang 1997. *Bounding models for estimating changes in fracture permeability due to thermo-mechanical stresses in host rock surrounding the repository. I: Permeability changes estimated for the Heated Drift Test.* (SPLF2M4) Livermore, California: Lawrence Livermore National Laboratory.

Blair, S. C., T. A. Buscheck, E. Carlberg, R. Carlson, M. S. Costantino, W. D. Daily, L. D. DeLoach, K. Lee, W. Lin, R. Pletcher, A. L. Ramirez, J. J. Roberts, N. D. Rosenberg, D. Ruddle & J. L. Wagoner 1998. *Drift-Scale Test status report.* (SP2670M4 and SP2931M4) Livermore, California: Lawrence Livermore National Laboratory.

Bodvarsson, G. S. & T. M. Bandurraga 1996. *Development and calibration of the three-dimensional Site-Scale Unsaturated Zone Model of Yucca Mountain, Nevada.* (LBNL-39315) Berkeley, California: Lawrence Berkeley National Laboratory, Earth Sciences Division.

Bodvarsson, G. S., T. M. Bandurraga & Y. S. Wu 1997. *The Site-Scale Unsaturated Zone Model of Yucca Mountain, Nevada, for the Viability Assessment.* (LBNL-40376, UC-814) Berkeley, California: Lawrence Berkeley National Laboratory, in collaboration with U.S. Geological Survey.

Brown, S. R. 1994. *Simple mathematical model of a rough fracture.* (SAND92-2216J) Albuquerque, New Mexico: Sandia National Laboratories.

Brown, S. R. 1995. Simple mathematical model of a rough fracture. *J. Geophys. Res.* 100:5941–5952.

Brown, S. R. & R. L. Bruhn 1997. *Fluid permeability of deformable fracture networks.* (SAND97-0159) Albuquerque, New Mexico: Sandia National Laboratories.

Hardin, E. L., S. C. Blair, T. A. Buscheck, D. A. Chesnut, L. D. DeLoach, W. E. Glassley, J. W. Johnson, R. B. Knapp, K. Lee, A. Meike, K. Myers, J. J. Nitao, C. E. Palmer, L. L. Rogers, N. D. Rosenberg, B. E. Viani, H. F. Wang, C. Wittwer & T. J. Wolery 1998. *Near-field/altered-zone models report.* (UCRL-ID-129179) Livermore, California: Lawrence Livermore National Laboratory.

Hardin, E. L. & D. A. Chesnut 1997. *Synthesis report on thermally driven coupled processes.* (SPL8BM3) Livermore, California: Lawrence Livermore National Laboratory.

Itasca Consulting Group Inc. *FLAC^{3D}: Fast Lagrangian Analysis of Continua, version 2.0, vol. I-IV, user's manuals.* Minneapolis, Minnesota: Itasca Consulting Group, Inc.

Jaeger, J. C. & N. G. W. Cook. *Fundamentals of rock mechanics.* London, United Kingdom: Chapman and Hall.

Nitao, J. J. 1998a. *Reference manual for the NUFT flow and transport code, version 2.0.* (UCRL-MA-130651) Livermore, California: Lawrence Livermore National Laboratory.

Nitao, J. J. 1998b. *User's manual for the USNT module of the NUFT code, version 2.0 (NP-phase, NC-component, thermal).* (UCRL-MA-130653) Livermore, California: Lawrence Livermore National Laboratory.

Ouyang, Z. & D. Elsworth 1993. Evaluation of groundwater flow into mined panels. *Int. J. Rock Mech. Min. Sci. & Geomech. Abs*. 30(2):71–79.

Stock, J. M., J. H. Healy & S. H. Hickman 1984. *Report on televiewer log and stress measurements in Core Hole USW G-2, Nevada Test Site.* (OFR-84-172) Denver: U.S. Geological Survey.

Stock, J. M., J. H. Healy, S. H. Hickman & M. D. Zoback 1985. Hydraulic fracturing stress measurements at Yucca Mountain, Nevada, and relationship to regional stress field. *J. Geophys. Res.* 90(B10):8691–8706.

Turcotte, D. L. & G. Schubert. *Geodynamics applications of continuum physics to geological problems.* New York: Wiley.

Wilder, D. G. 1987. *Influence of stress-induced deformations on observed water flow in fractures at the climax granitic stock.* (UCRL-95539, Rev. 1) Livermore, California: Lawrence Livermore National Laboratory.

Work performed under the auspices of the U.S. Department of Energy by the Lawrence Livermore National Laboratory under Contract W-7405-Eng-48.